

Article

Experimental Investigation of Triboelectrification Behaviour in the Friction Process

Guobin Li ¹, Sifan Yang ¹, Pengfei Xing ^{1,*} , Ting Liu ^{2,*}, Honglin Gao ¹, Yuchao Song ¹ and Hongpeng Zhang ¹ ¹ Marine Engineering College, Dalian Maritime University, Dalian 116026, China² College of Mechanical and Electronic Engineering, Dalian Minzu University, Dalian 116600, China

* Correspondence: wlyxpf@dlnu.edu.cn (P.X.); liuting@dlnu.edu.cn (T.L.)

Abstract: The triboelectrification phenomenon can occur during the friction process of metal contact pairs. An in-depth understanding of triboelectrification behaviour is incredibly beneficial to controlling friction and wear. However, due to the complexity of the driving mechanism, it is still challenging to gain a thorough understanding of the triboelectrification behaviour of metal–metal contact pairs. To further reveal the triboelectrification behaviour during the friction process of metal pairs, wear experiments of GCr15 steel–cast iron were carried out on a CFT-I tribometer under oil-free and oil lubrication conditions. The triboelectric current signal was collected during the investigation, and its variation was discussed. The result shows that the varying trend of the triboelectric current was consistent with that of the friction coefficient in the friction process. The triboelectrification of similar metal contact pairs primarily driven by material transfer was closely related to friction and wear conditions.

Keywords: experimental investigation; friction; triboelectrification; driving mechanism



Citation: Li, G.; Yang, S.; Xing, P.; Liu, T.; Gao, H.; Song, Y.; Zhang, H. Experimental Investigation of Triboelectrification Behaviour in the Friction Process. *Lubricants* **2022**, *10*, 180. <https://doi.org/10.3390/lubricants10080180>

Received: 2 July 2022

Accepted: 5 August 2022

Published: 9 August 2022

Publisher's Note: MDPI stays neutral with regard to jurisdictional claims in published maps and institutional affiliations.



Copyright: © 2022 by the authors. Licensee MDPI, Basel, Switzerland. This article is an open access article distributed under the terms and conditions of the Creative Commons Attribution (CC BY) license (<https://creativecommons.org/licenses/by/4.0/>).

1. Introduction

It is well-known that triboelectrification occurs during the friction process of friction pairs [1–4]. Understanding and ultimately controlling triboelectrification could have wide applications in the field of tribology, such as wear monitoring and friction suppression [5,6]. Therefore, an in-depth understanding of triboelectrification behaviour is incredibly beneficial to controlling friction and wear.

Triboelectrification results from transferring charge from one object to another in the friction process [7,8]. To explain this phenomenon, some driving mechanisms of charge transfer have been proposed, such as separation charging, the Seebeck effect, and material transfer [9]. The separation charging is mainly attributed to the separation of contacting surfaces, which can be neglected under a complete contact condition of the friction pair. The Seebeck potential is caused by the temperature difference between a metal pair [10], which is referred to as charging by a Seebeck effect. Considering the Seebeck effect, the reciprocating speed and the normal load on the triboelectrification mechanism were investigated for the five soft metals (Pb, Ag, Cu, Zn, and Al), sliding on iron for complete contact under severe dry wear in a reciprocating friction process [11,12]. The results show that the triboelectrification resulted mainly from the Seebeck effect at an average sliding velocity higher than 200 mm/s and the Seebeck potential was linear with the reciprocating speed. Moreover, the influence of material transfer cannot be ignored, especially at low speeds. Wear debris appears when the asperities of a contact surface are removed from an original surface due to strong adhesion. It is attached to the opposite surface, transferring material from one surface to the other. Since free electrons are excited during the material transfer, some scholars believe the material transfer could cause the charging. Furthermore, the triboelectrification behaviour was investigated for self-mated pure hard and soft metal pairs in a dry severe wear process [13,14]. The results show that the material transfer influenced the polarity of triboelectrification in the friction process

of metal friction pairs. On this basis, the triboelectrification behaviour caused by material transfer was investigated in the same metal friction pairs of different wear mechanisms [15]. A micro-model of the triboelectrification mechanism for self-mated materials was proposed to explain the intermittent positive and negative polarity of the same material in the wear process [16]. Furthermore, triboelectrification was successfully applied to monitor the tribological properties of the metal films [17].

The above research shows that triboelectrification is closely related to the friction and wear of friction pairs, and its behaviour is distinct under different tribological conditions. However, due to the complexity of the driving mechanism, it is still challenging to gain a comprehensive understanding of triboelectrification. In fact, triboelectrification is a consequence of combining different mechanisms in sequence or parallel, leading to the triboelectrification source of charge and transfer form being unrevealed. Therefore, it is still challenging to gain a thorough understanding of triboelectrification, and the interaction between triboelectrification and friction needs further investigation to push our understanding forward.

In this study, the triboelectrification experiments were conducted on a ball-on-disk tribometer, and the triboelectric current signals were measured in the experiment process. Based on the measured triboelectric current signals, the triboelectrification behaviours under different friction states were investigated, and their driving mechanism was discussed.

2. Experiments

2.1. Experimental Apparatus

As shown in Figure 1, the experiments were conducted on a triboelectrification test bench consisting of a signal analysis system and a tribometer. During the investigation, the triboelectric current signals were obtained by the signal analysis system consisting of an electrometer, a data acquisition system, and a computer. To obtain the weak triboelectric current signal, an electrometer (model Keithley 6514, USA) with a resolution of 100 nA in the range of 20 mA and a resolution of 100 pA in the range of 20 μ A and a data acquisition system (model NI-9215, USA) with a sampling rate of 100 ks/s were selected.

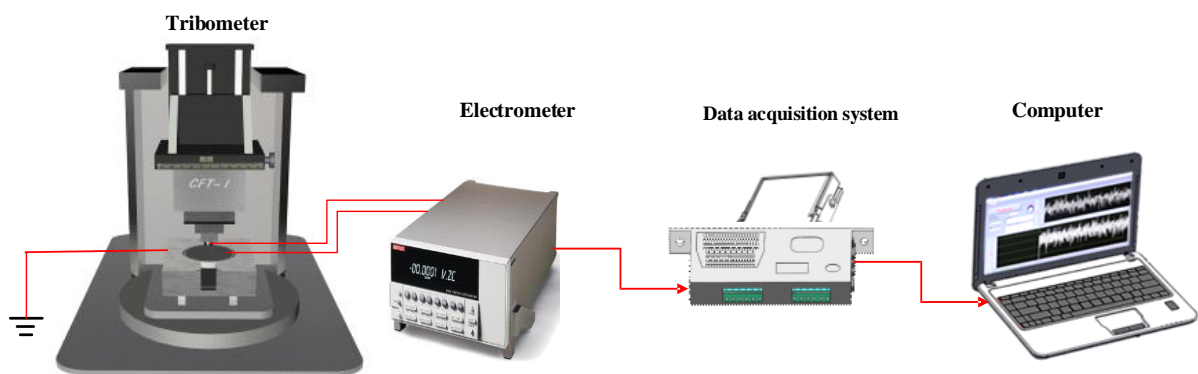


Figure 1. Triboelectrification test bench.

The ball-on-disk wear experiments were carried out using a reciprocating tribometer (model CFT-I, China). The ball and disk specimens were connected to the negative and positive electrodes of the electrometer by wires, respectively. Moreover, to measure the triboelectric current, the ball and disk specimens were insulated from the tribometer by an insulation gasket, as shown in Figure 2. The ball specimen was mounted under the load device, which can apply a normal load in the 0–200 N range at a rate of 0.1 N/s, and kept stationary in the wear process. The disk specimen was driven in a reciprocating motion with a stroke of 5 mm by a crank–slider mechanism. The mechanism was connected to a motor with a rotational speed of 0–2000 rpm. Two force sensors were equipped for measuring the normal load and the friction force between the ball and disk specimens.

The friction coefficient could be calculated in real-time by the data processing system of the tribometer.

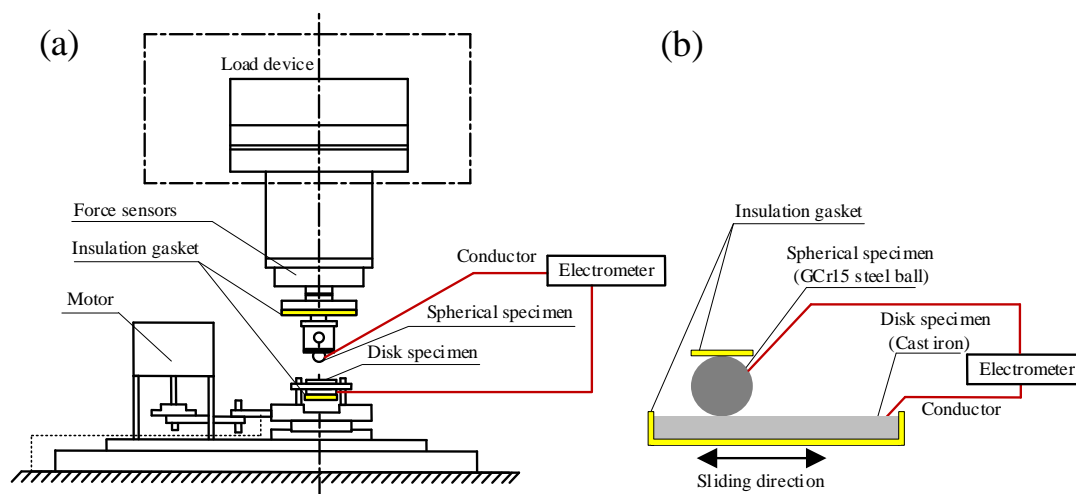


Figure 2. Schematic diagram of the tribometer: (a) a testing machine, (b) friction pair.

2.2. Friction Pair

Ball and disk specimens were used as tribological pairs, as depicted in Figure 2b. Specifically, the ball specimen was made of GCr15 steel with 750 HV hardness, a $\Phi 6$ mm diameter, and surface roughness $S_a = 0.125 \mu\text{m}$. Moreover, the disk specimen was cast iron with 350 HV hardness, 16 mm diameters, and a surface roughness $S_a = 0.73 \mu\text{m}$.

2.3. Experimental Set-Up

The wear experiments were performed under oil-free and oil lubrication conditions, respectively. The motor drove the disk specimen at a speed of 400 rpm. The average relative sliding velocity between the ball and disk was 0.067 m/s. The pressure load applied on the ball specimen was 20 N and 100 N under oil-free and oil lubrication conditions, respectively, and each experiment lasted for 14 min. In the oil lubrication experiment, the submerged lubrication was conducted using CD40 (a standard marine lube oil) with a density of 0.8957 g/cm^3 and a viscosity of 139.6 cSt at 40°C and 12.5 cSt at 100°C . The experiments were repeated seven times under the same conditions with different test durations of 2 min, 4 min, 6 min, 8 min, 10 min, 12 min, and 14 min to ensure good repeatability. The experimental set-up was designed with consideration of the fact that the accuracy of the experimental results would be influenced if the wear process were to be interrupted.

2.4. Acquisition of Data

The triboelectric current signals were collected with 3072 sampling points and a sampling interval of 1.95 ms. A set of triboelectric current signals was collected during the experiments every 60s. Under the oil-free and oil lubrication conditions, 14 groups of triboelectric current signals were obtained. To avoid the interruption of externally induced electricity, the tribometer was grounded. Furthermore, the 3-D surface topography of the friction pair was measured using a confocal laser scanning microscope (model OLS4000, Tokyo, Japan) before and after experiments.

3. Results and Discussions

3.1. Change in Triboelectric Current under Different Lubrication Conditions

3.1.1. Oil-Free Lubrication

The triboelectric current signals collected after accomplishing the loading process of the CFT-I tribometer were taken as the representatives of the corresponding minute. The time-domain waveforms of the triboelectric current signals collected under oil-free

lubrication are shown in Figure 3. It can be seen from Figure 3a–f that despite the similar waveforms of triboelectric current signals, their amplitudes at different times were distinct, which implies that triboelectrification varies with the friction state. To investigate the relationship between the triboelectrification and the friction state, the mean values of triboelectric current signals at different times were calculated. Figures 4 and 5 depict the change in the triboelectric current signal and friction coefficient, respectively. It can be seen from the comparison of Figures 4 and 5 that both the triboelectric current and the friction coefficient went through three different stages: the sharply rising stage, the slowly dropping stage, and the smoothly fluctuating stage, which indicates that the triboelectric current and the friction coefficient had the same changing trend, and the triboelectrification is closely related to the friction state.

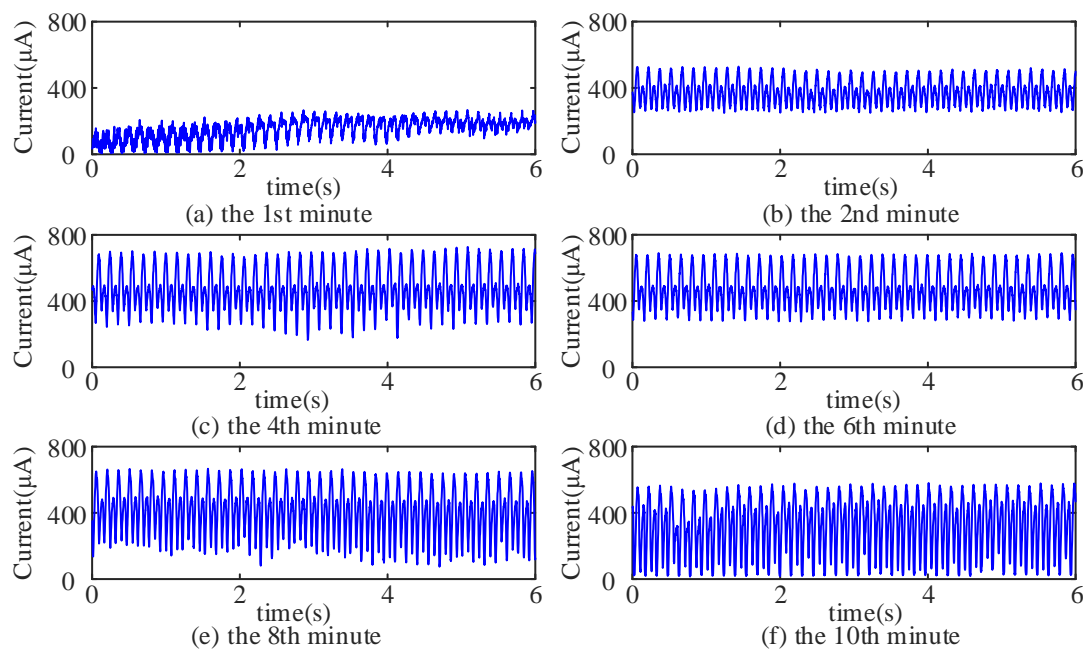


Figure 3. Time-domain waveform of triboelectric current under oil-free lubrication.

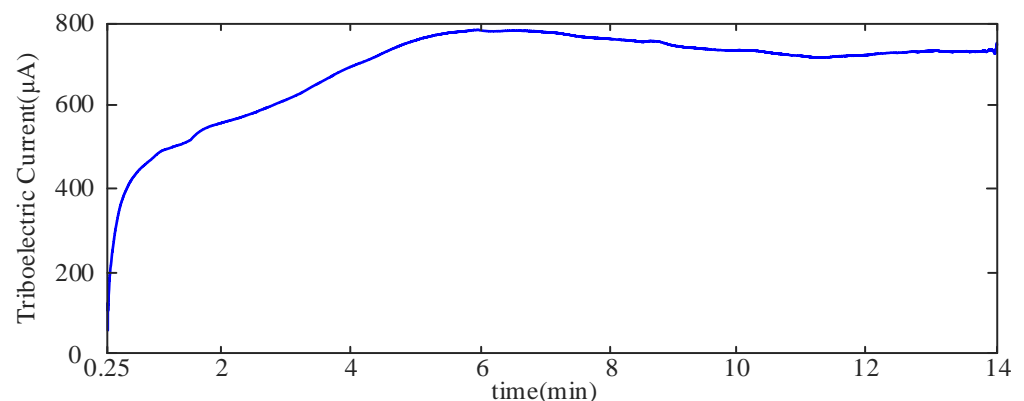


Figure 4. Change in triboelectric current with time under oil-free lubrication.

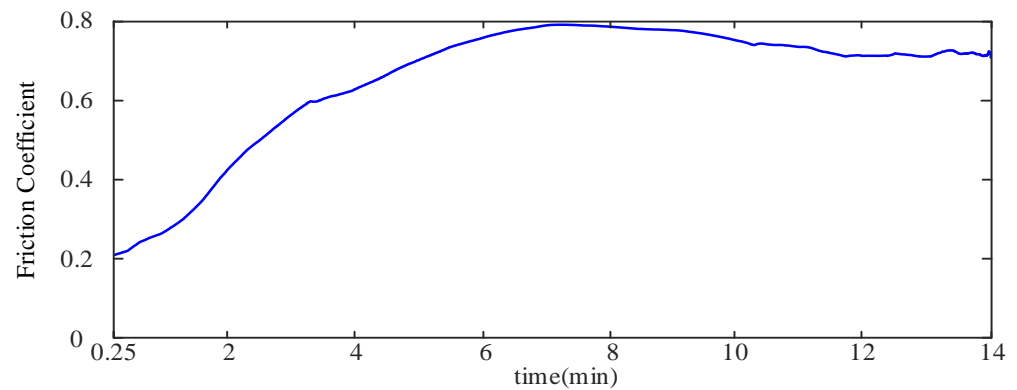


Figure 5. Change in friction coefficient with time under oil-free lubrication.

3.1.2. Oil Lubrication

The time-domain waveforms of the triboelectric current signals under oil lubrication conditions are shown in Figure 6. The amplitudes of current signals at different times were also distinct. Furthermore, the mean values of triboelectric current signals and the friction coefficient at different times were obtained separately. The changes with time are separately shown in Figures 7 and 8. It can be observed that the triboelectric current and the friction coefficient also had the same changing trend, which indicates that under oil lubrication conditions, the triboelectrification is also closely related to the friction state. However, the trend of triboelectric current under oil lubrication was different from that under oil-free lubrication; it shows the change of first decreasing and then tending to steady. In addition, the amplitude of the triboelectric current signal under oil lubrication was much smaller than under oil-free lubrication. The difference in triboelectric current signals between oil lubrication and oil-free lubrication conditions further proves that triboelectrification is closely related to the friction state.

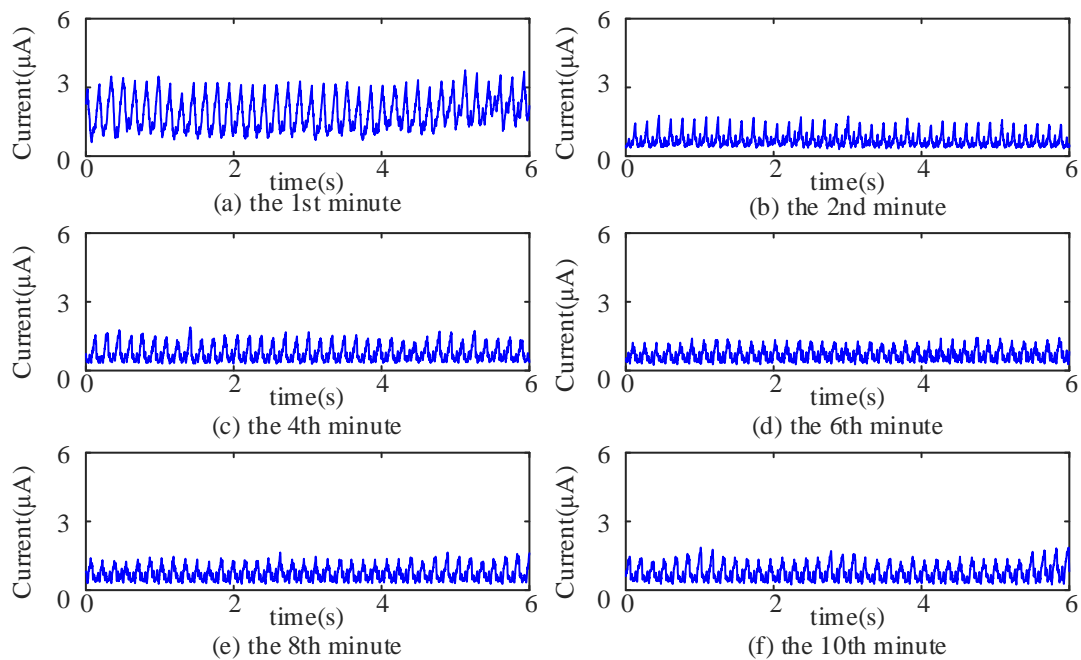


Figure 6. Time-domain waveform of triboelectric current under oil lubrication.

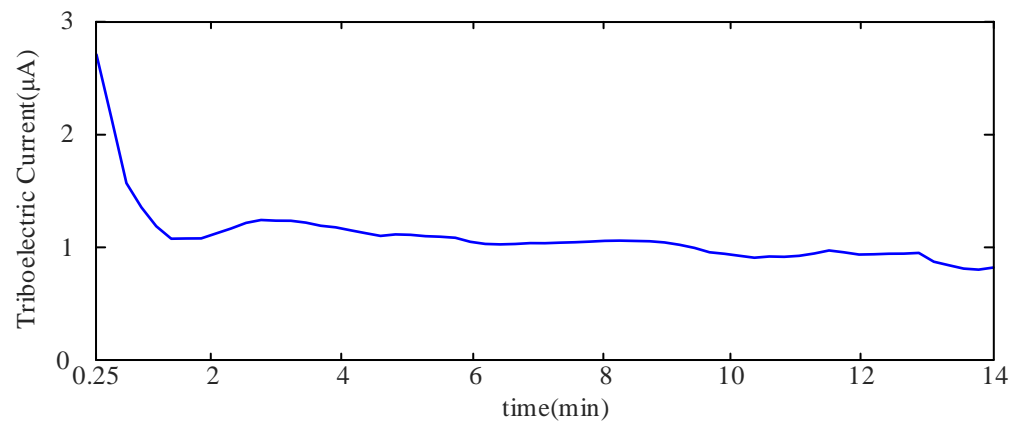


Figure 7. Change in triboelectric current with time under oil lubrication.

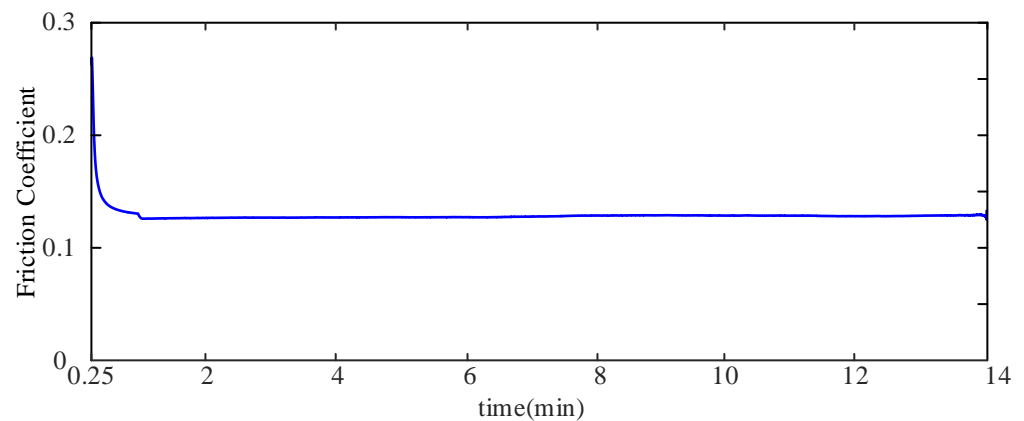


Figure 8. Change in friction coefficient with time under oil lubrication.

As discussed above, the change in the triboelectric current signal presents a trend consistent with that of the friction coefficient during the friction process of the friction pair, which indicates that the triboelectrification is closely related to the friction state. However, the driving mechanism of triboelectrification still needs to be further discussed.

3.2. Driving Mechanism of Triboelectrification

In this study, two similar types of metals, carbon steel and cast iron, were selected as the friction pairs and were always kept in contact during the experiment. According to the reference [13], the Seebeck effect can be neglected for similar metal pairs, such as Fe–Steel. In addition, because the metal friction–pair was under complete-contact conditions, the electrical charge from separation was neglected [11]. Thus, the material transfer is regarded as the dominant factor of triboelectrification under full-contact conditions of similar metal pairs. Due to the material transfer being closely related to the wear mechanism in a wear process [18], the material transfer under different friction conditions is discussed in view of a transition of the wear mechanism and severity.

3.2.1. Material Transfer Characteristics under Oil-Free Lubrication

The material loss mainly occurred on the disk specimen because its hardness (350HV) was far lower than that of the ball specimen (750HV). Thus, the effect of the material transfer is discussed by examining the surface topographies of the disk specimen. Figure 9 presents the surface topographies and wear scar profile curves of disk specimens at different times. It can be seen that there were many machining marks on the specimen surface before the wear, as shown in Figure 9I. After two minutes into the wear experiment, small plastic deformation and particle exfoliation appeared on the wear scar area, and a wear scar with

a depth of $9.7\ \mu\text{m}$ was observed, as shown in Figure 9II. The characteristics of the wear scar indicate that adhesive wear accompanied by mild abrasive wear was the primary wear mechanism, and it dominated the occurrence of material transfer. As the wear experiment continued, the particle exfoliation increased and the wear scar became deeper, as shown in Figure 9III. When the wear experiment had continued for 6 min, large plastic deformation occurred in the wear scar of about $17.3\ \mu\text{m}$ in depth, as shown in Figure 9IV. The wear mechanism was adhesive wear accompanied by abrasive wear, which indicates that the material transfer increased significantly. After the eighth minute, the particle exfoliation and plastic deformation began to decrease. The wear scar became smooth, and its depth no longer increased significantly, as shown in Figure 9V,VI. The above phenomena indicate that the disk specimen entered a steady wear stage, and the material transfer became stable. In conclusion, the material transfer of the disk specimen presents a trend of increasing, decreasing, and then tending to be stable under oil-free lubrication. Therefore, the triboelectrification driven by the material transfer also presents the same trend, as shown in Figure 6.

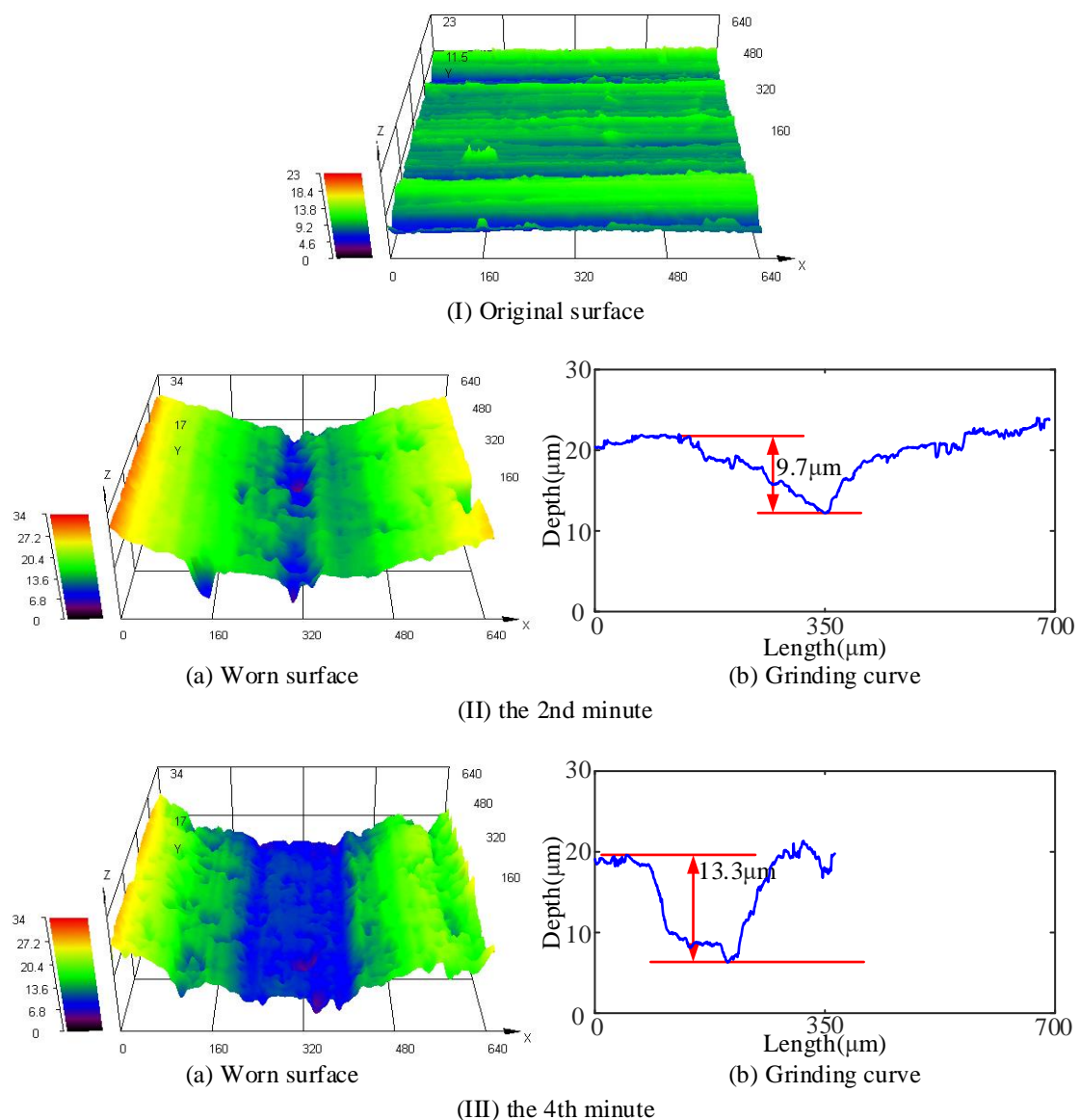


Figure 9. Cont.

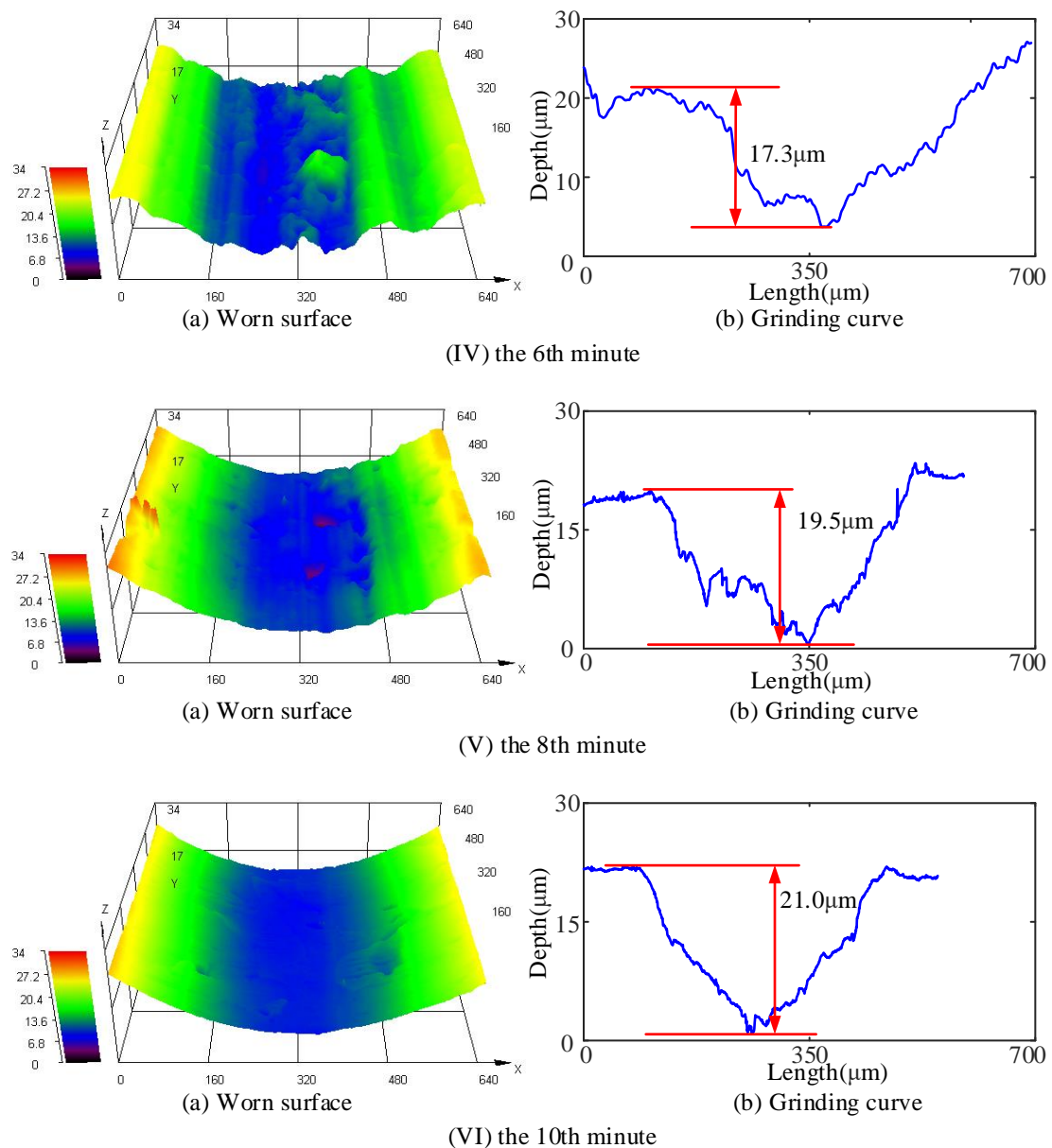


Figure 9. Surface topographies and wear scar profile curves of disk specimen under oil-free lubrication.

3.2.2. Material Transfer Characteristics under Oil Lubrication

Figure 10 presents the surface topographies and wear scar profile curves of disk specimens at different times under oil lubrication. It can be seen that the surface of the disk specimen was relatively rough before the test due to the existence of machining marks. As the wear experiment continued, the machining marks on the surface were gradually worn away to form a smooth, worn region, as shown in Figure 10II(a)–IV(a). At the same time, the wear scar gradually became deeper, as shown in Figure 10II(b)–IV(b). Compared with oil-free lubrication, the wear scar depth was reduced under oil lubrication, which means that the material transfer of the disk specimen under oil lubrication was smaller than that under oil-free lubrication. Therefore, the triboelectrification driven by the material transfer under oil lubrication was significantly reduced, as shown in Figure 7.

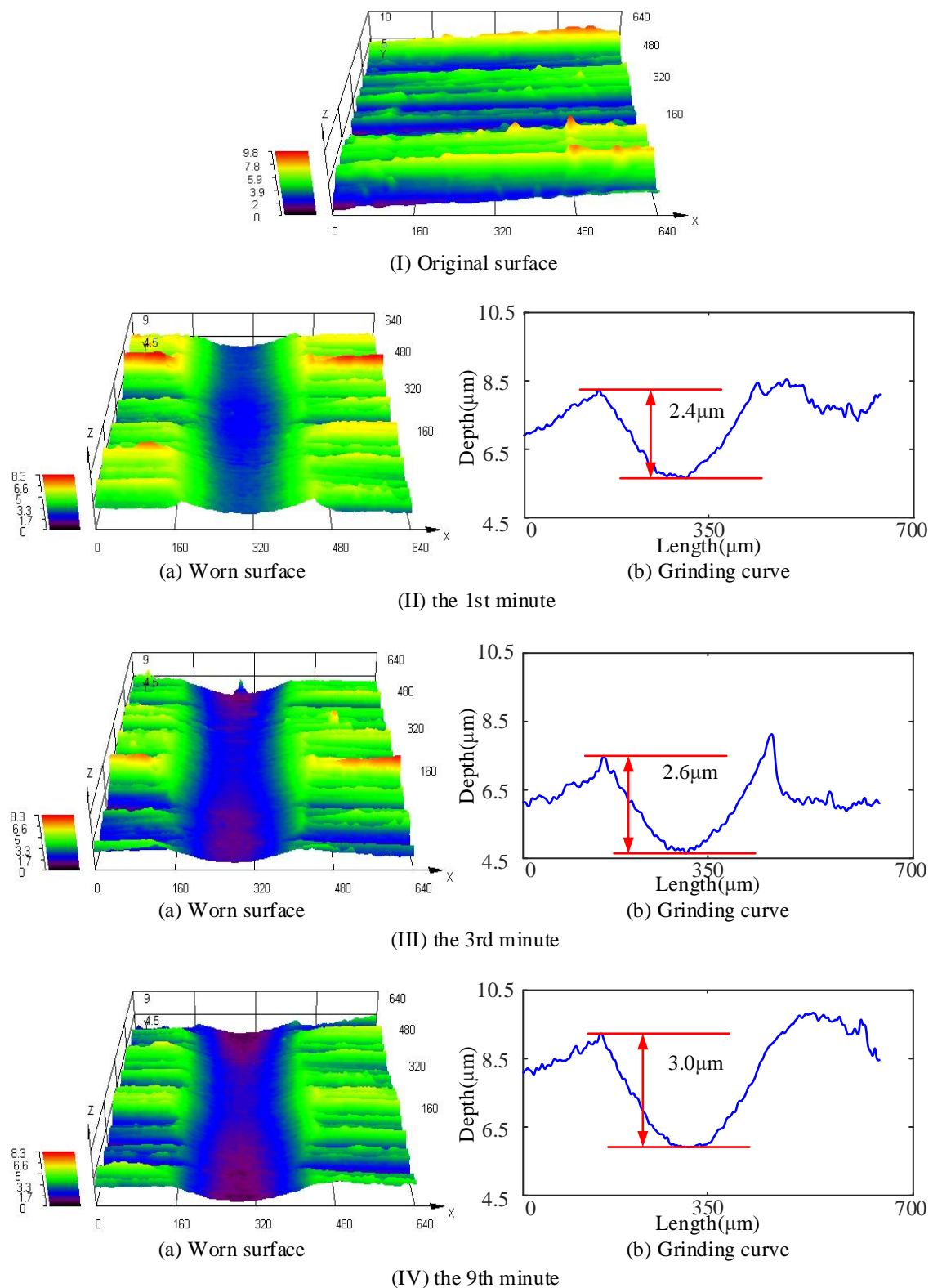


Figure 10. Surface topographies and wear scar profile curves of disk specimen under oil lubrication.

As mentioned above, the triboelectrification driven by material transfer could be related to the friction condition and wear severity in the friction and wear process. However, due to the complexity of friction and wear, the correspondence between triboelectrification, friction, and wear still needs further investigation.

4. Conclusions

The triboelectrification behaviours of similar metal pairs and their driving mechanism were investigated based on friction and wear experiments under oil-free and oil lubrication conditions. The following conclusions can be obtained:

1. The triboelectric current presented a trend consistent with the friction coefficient, which indicates that triboelectrification is closely related to the friction condition.
2. Triboelectrification driven by material transfer is related to wear severity. The more severe the wear, the larger the triboelectric current. The less severe the wear, the smaller the triboelectric current.

Author Contributions: Conceptualization, G.L., T.L. and H.Z.; data curation, S.Y.; formal analysis, G.L., S.Y. and Y.S.; funding acquisition, G.L., P.X. and T.L.; investigation, T.L., H.G. and H.Z.; methodology, G.L.; software, S.Y., P.X., H.G. and Y.S.; supervision, G.L.; visualization, P.X.; writing—original draft, G.L. and S.Y.; writing—review and editing, G.L. and P.X. All authors have read and agreed to the published version of the manuscript.

Funding: This research was funded by the Fundamental Research Funds for the Central Universities grant number 3132022222, the National Natural Science Foundation of China grant number 51879020 and the High-level talent innovation support program Youth Science and technology star project grant number 2021RQ133.

Institutional Review Board Statement: Not applicable.

Informed Consent Statement: Not applicable.

Data Availability Statement: The data presented in this study are available on request from the corresponding author.

Acknowledgments: We appreciate each of the anonymous reviewers for their valuable comments and suggestions for improving the quality of this paper.

Conflicts of Interest: The authors declare no conflict of interest.

References

1. Pan, S.; Yin, N.; Zhang, Z. Time- & load-dependence of triboelectric effect. *Sci. Rep.* **2018**, *8*, 2470. [[PubMed](#)]
2. Pan, S.; Zhang, Z. Fundamental theories and basic principles of triboelectric effect: A review. *Friction* **2019**, *7*, 2–17. [[CrossRef](#)]
3. Zhang, Z.; Yin, N.; Wu, Z.; Pan, S.; Wang, D. Research methods of contact electrification: Theoretical simulation and experiment. *Nano Energy* **2021**, *79*, 105501. [[CrossRef](#)]
4. Lacks, D.J.; Shinbrot, T. Long-standing and unresolved issues in triboelectric charging. *Nat. Rev. Chem.* **2019**, *3*, 465–476. [[CrossRef](#)]
5. Zhang, Y.; Shao, T. A method of charge measurement for contact electrification. *J. Electrostat.* **2013**, *71*, 712–716. [[CrossRef](#)]
6. Zhang, Y.; Shao, T. Contact electrification between polymers and steel. *J. Electrostat.* **2013**, *71*, 862–866. [[CrossRef](#)]
7. Burgo, T.A.; Silva, C.A.; Balestrin, L.; Galembeck, F. Friction coefficient dependence on electrostatic tribocharging. *Sci. Rep.* **2013**, *3*, 2384. [[CrossRef](#)] [[PubMed](#)]
8. Burgo, T.A.; Ducati, T.R.; Francisco, K.R.; Clinckspoor, K.J.; Galembeck, F.; Galembeck, S.E. Triboelectrification: Macroscopic charge patterns formed by self-arraying ions on polymer surfaces. *Langmuir* **2012**, *28*, 7407–7416. [[CrossRef](#)] [[PubMed](#)]
9. Harper, W.R. *Contact and Frictional Electrification*; Oxford University Press: London, UK, 1967; pp. 44–51, 73–75, 223–225.
10. Zhang, Z.; He, T.; Zhao, J.; Liu, G.; Wang, Z.L.; Zhang, C. Tribo-thermoelectric and tribovoltaic coupling effect at metal-semiconductor interface. *Mater. Today Phys.* **2021**, *16*, 100295. [[CrossRef](#)]
11. Chang, Y.; Chiou, Y.; Lee, R. Tribo-electrification mechanisms for dissimilar metal pairs in dry severe wear process: Part I. Effect of speed. *Wear* **2008**, *264*, 1085–1094. [[CrossRef](#)]
12. Chang, Y.; Chiou, Y.; Lee, R. Tribo-electrification mechanisms for dissimilar metal pairs in dry severe wear process: Part II. Effect of load. *Wear* **2008**, *264*, 1095–1104. [[CrossRef](#)]
13. Chiou, Y.; Chang, Y.; Lee, R. Tribo-electrification mechanism for self-mated metals in dry severe wear process: Part I. Pure hard metals. *Wear* **2003**, *254*, 606–615. [[CrossRef](#)]
14. Chiou, Y.; Chang, Y.; Lee, R. Tribo-electrification mechanism for self-mated metals in dry severe wear process: Part II: Pure soft metals. *Wear* **2003**, *254*, 616–624. [[CrossRef](#)]
15. Chang, Y.; Chiou, Y.; Lee, R. The transition mechanisms of tribo-electrification for self-mated metals in dry severe wear process. *Wear* **2004**, *257*, 347–358. [[CrossRef](#)]
16. Chang, Y.; Chu, H.; Chou, H. Effects of mechanical properties on the tribo-electrification mechanisms of iron rubbing with carbon steels. *Wear* **2007**, *262*, 112–120. [[CrossRef](#)]

-
17. Chang, Y.P. A novel method of using continuous tribo-electrification variations for monitoring the tribological properties between pure metal films. *Wear* **2007**, *262*, 411–423. [[CrossRef](#)]
 18. Wen, S.Z.; Huang, P. *Principles of Tribology*; Tsinghua University Press: Beijing, China, 2008.